Article:
Li, W., Cai, J., Cai, F. et al. (6 more authors) (2018) Achieving over 11% power conversion efficiency in PffBT4T-2OD-based ternary polymer solar cells with enhanced open-circuit-voltage and suppressed charge recombination. Nano Energy, 44. pp. 155-163. ISSN 2211-2855

https://doi.org/10.1016/j.nanoen.2017.12.005

Achieving over 11% power conversion efficiency in PffBT4T-2OD-based ternary polymer solar cells with enhanced open-circuit-voltage and suppressed charge recombination

Wei Li[1,2], Jinlong Cai[1,2], Feilong Cai[1,2], Yu Yan[1,2], Hunan Yi[3], Robert S. Gurney[1,2], Dan Liu[1,2], Ahmed Iraqi[3], David G. Lidzey[4], Tao Wang[1,2]*

[1]School of Materials Science and Engineering, Wuhan University of Technology, Wuhan 430070, China E-mail: twang@whut.edu.cn

[2]State Key Laboratory of Silicate Materials for Architectures, Wuhan University of Technology, Wuhan 430070, China

[3]Department of Chemistry, University of Sheffield, Sheffield S3 7HF, UK

[4]Department of Physics and Astronomy, University of Sheffield, Sheffield S3 7RH, UK

Determination of the location of the PCDTBT8 in PffBT4T-2OD:$PC_{71}BM$ blends via surface energy analysis

The localization of the third component in ternary blends can be inferred from the interfacial surface energy and wetting coefficient of the third component. The interfacial surface energy between different materials in the blend can be further calculated using the followed equation 3, where γ x-y is the interfacial surface energy between component X and Y, and β =0.000115 $m^4/mJ2$. The wetting coefficient of the third component in the blend can be calculated using Young's equation expressed in equation 4. If $\omega_{\text{Third component}} > 1$, the third component will locate in the PTB7-Th domain. If $1 > \omega_{\text{Third component}} > -1$, the third component will locate at the interface between PTB7-Th and $PC_{71}BM$. If $\omega_{\text{Third component}} < -1$, the third component will locate in the $PC_{71}BM$ domain.

$$\gamma_{x-y} = \gamma_x + \gamma_y - 2\sqrt{\gamma_x * \gamma_y}\, e^{[-\beta(\gamma_x-\gamma_y)^2]} \quad (1)$$

$$\omega = \frac{\gamma_{\text{third component}-PC_{71}BM} - \gamma_{\text{third component}-\text{PffBT4T}-2OD}}{\gamma_{\text{PffBT4T}-2OD-PC_{71}BM}} \quad (2)$$

Table S1 Surface energy of PffBT4T-2OD, PCDTBT8 and $PC_{71}BM$.

	PffBT4T-2OD	PCDTBT8	$PC_{71}BM$
Surface energy ($mJ\ cm^{-2}$)	18.5	21.6	35.5

Table S2 Interfacial surface energy between components x and y in different blends.

	PffBT4T-2OD :PCDTBT8	$PC_{71}BM$: PCDTBT8	PffBT4T-2OD :$PC_{71}BM$
$\gamma_{x\text{-}y}$:	0.16	2.93	1.21

Table S3 Wetting coefficient of PCDTBT8 in PffBT4T-2OD:$PC_{71}BM$ blend

	PCDTBT8 in PffBT4T-2OD:$PC_{71}BM$
Wetting coefficient	0.63

GISAXS modeling

To quantify and compare the phase separation in the binary and ternary photovoltaic blends, the 1D GISAXS profiles were fitted using a universal model expressed in Equation 1 using the fitting software SasView (Version 3.1.2). The first term of the equation is the so-called Debye−Anderson−Brumberger (DAB) term, which can model the scattering of dispersed $PC_{71}BM$ particles within the polymer domain in the low q range up to 0.008 $Å^{-1}$, where q is the scattering wave vector, A_1 is an independent fitting parameter, and ξ is the average correlation length of the fullerene dispersed polymer domain. The second term represents the contribution from fractal-like aggregations of $PC_{71}BM$. Here, P(q, R) is the form factor of $PC_{71}BM$. S(q, R, η, D) is the fractal structure factor, which describes the interaction between primary particles in this fractal-like aggregation system, with R the mean spherical radius of primary $PC_{71}BM$ particles, and η the correlation length of the fractal-like structure. The average domain size of the clustered fullerene phases is approximately characterized by the Guinier radius (R_g) of the network, where $R_g = \sqrt{\left(\frac{D(D+1)}{2}\right)}\,\eta$.

$$I(q) = \frac{A_1}{[1+(q\xi)^2]^2} + A_2\langle P(q, R)\rangle S(q, R, \eta, D)+B \qquad (1)$$

$$S(q) = 1 + \frac{\sin[(D-1)\tan^{-1}(q\eta)]}{(qR)^D}\, b\pm\sqrt{b^2-4ac}\, \frac{D\Gamma\,(D-1)}{\left[1+\frac{1}{(q\eta)^2}\right]^{(D-1)/2}} \qquad (2)$$

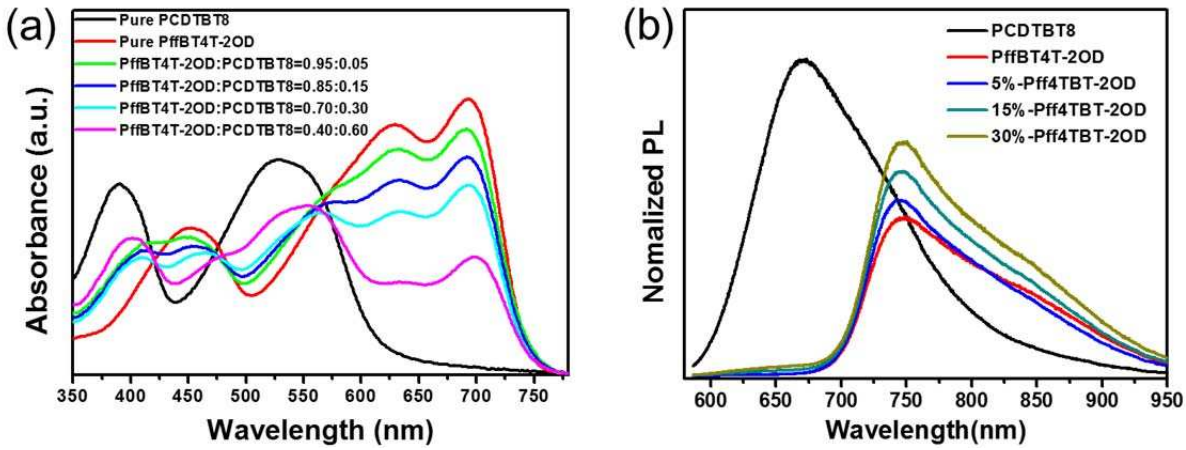

Figure S1 (a) PL and (b) Absorption spectra of PffBT4T-2OD films with the addition of different amount of PCDTBT8.

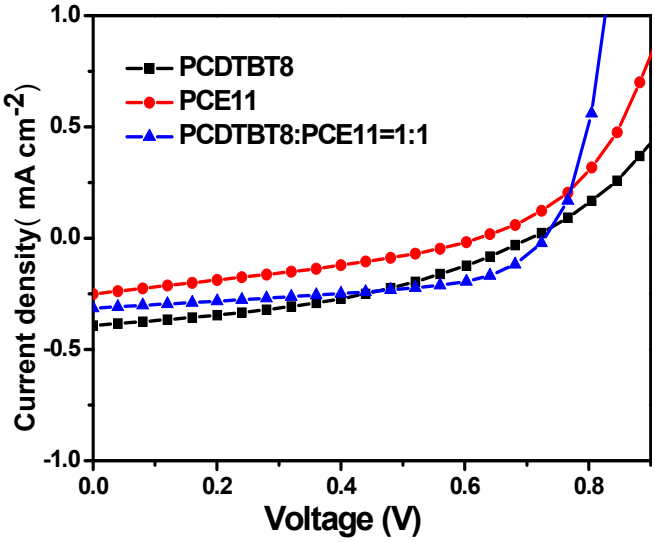

Figure S2 J-V curves of PffBT4T-2OD:PCDTBT8 binary solar cells with different blending ratios measured under AM1.5G illumination at 100 mW cm^{-2}.

Table S4 Summary of photovoltaic parameters of inverted ternary solar cells with different contents of PCDTBT8 and $PC_{71}BM$ under the illumination of AM 1.5G at 100 mW cm^{-2}. The data presented are the maximum values followed with average values and standard deviations in the parentheses obtained from over 20 individual devices. The size of the active area of each device pixel is 2.12 mm^2.

PffBT4T2OD:PCDTBT8:$PC_{71}BM$	Voc [V]	Jsc [mA cm^{-2}]	FF [%]	PCE [%]
1:0:1.2	0.75 (0.75±0.01)	19.5 (19.2±0.3)	72.2 (71.8±0.6)	10.57 (10.3±0.12)
0.95:0.05:1.3	0.76 (0.76±0.01)	18.7 (18.2±0.4)	75.7 (75.2±0.4)	10.90 (10.8±0.11)
0.85:0.15:1.5	0.78 (0.78±0.01)	18.5 (18.0±0.7)	75.8 (75.4±0.5)	11.10 (11.2±0.60)
0.70:0.30:1.8	0.82 (0.82±0.01)	14.6 (14.4±0.2)	70.0 (69.1±0.9)	8.40 (8.3±0.30)

Table S5 Summary of photovoltaic parameters of inverted ternary solar cells with different contents of PCDTBT8 under the illumination of AM 1.5G at 100 mW cm^{-2}, with the size of the active area of 8.5 mm^2. The overall donors to $PC_{71}BM$ ratios were kept at 1:1.2.

PffBT4T2OD:PCDTBT8:$PC_{71}BM$	Voc [V]	Jsc [mA cm^{-2}]	FF [%]	PCE [%]
1:0:1.2	0.77 (0.77±0.01)	18.7 (18.5±0.5)	68.1 (67.5±0.8)	9.76 (9.6±0.18)
0.95:0.05:1.2	0.79 (0.79±0.01)	18.4 (18.2±0.6)	70.9 (70.6±0.6)	10.33 (10.2±0.26)
0.85:0.15:1.2	0.80 (0.80±0.01)	18.3 (18.1±0.5)	71.7 (70.9±1.1)	10.51 (10.4±0.23)
0.70:0.30:1.2	0.83 (0.83±0.01)	15.7 (15.5±0.4)	65.6 (65.1±0.8)	8.54 (8.3±0.22)

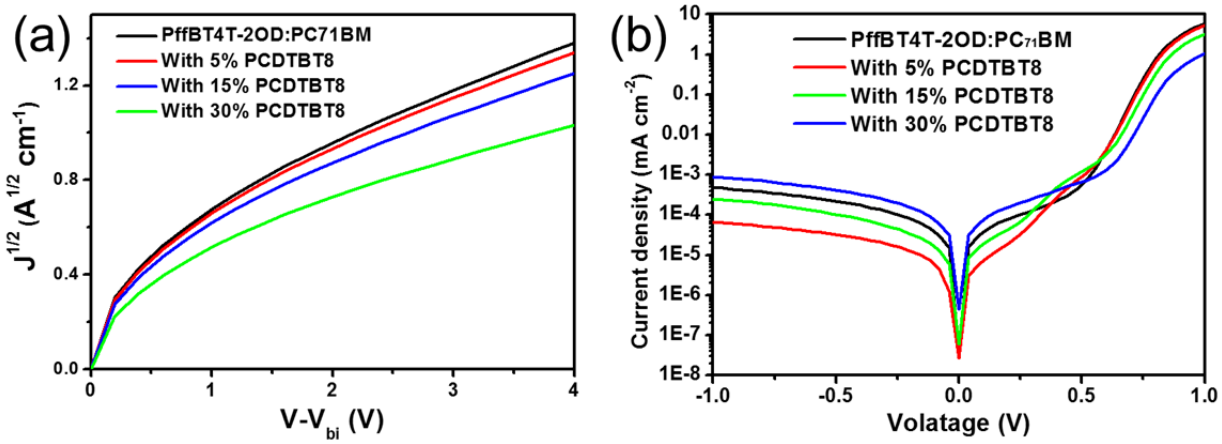

Figure S3 (a) Root square of hole current densities versus bias voltage of the ITO/PEDOT:PSS/Active layer/MoO_3/Ag hole-only devices, with the active layer having different contents of PCDTBT8. (b) J – V curves of ternary all-PSCs with different contents PCDTBT8 under dark condition.

Table S6 KT/q, Jsat, P(E,T) and hole mobility in binary and ternary OPVs.

	Jsat [mA cm^{-2}]	P(E,T) [%]	Hole mobility $cm^2V^{-1}S^{-1}$
PffBT4T-2OD:$PC_{71}BM$	19.9	97.9	0.0113
With 5% PCDTBT8	19.5	98.3	0.01027
With 15% PCDTBT8	19.2	98.0	0.0092
With 30% PCDTBT8	17.2	94.3	0.0058

Table S7 Summary of the electrical parameters of TSCs from Nyquist plots and equivalent circuit

	R_1 [Ω]	R_2 [Ω]	C [F]	R_3 [Ω]	CPE-P	CPE-T [F]	τ[μs]
PffBT4T-2OD:PC71BM	78.3	29.3	4.35 E-9	92.6	0.972	1.74 E-8	1.61
With 5% PCDTBT8	81.5	31.2	2.23 E-8	97.3	0.975	2.16 E-8	2.10
With 15% PCDTBT8	79.6	35.5	2.61 E-8	101.2	0.976	2.18 E-8	2.20
With 30% PCDTBT8	83.7	38.8	2.78 E-8	127.5	0.981	1.82 E-8	2.31

Calculation of V_{BI}, N from Mott – Schottky curves

The variation of C^{-2} under the dark with the applied bias voltage, measured at a frequency of 10 kHz. The built-in potential (V_{bi}) and impurity concentration (N) can be extracted from by the application of equation 3, where q is the elementary charge, ε_0 is the dielectric constant of vacuum, and ε is the relative dielectric constant of the semiconductor (assuming ε of 3). We estimated the values of V_{bi} by the voltage corresponding to the maximal of capacitance which equals the flat-band condition.

$$C^{-2} = \frac{2(V_{BI}-V_A)}{A^2 q\varepsilon\varepsilon_0 N} \quad (3)$$

Table S8 Summary of the Open-circuit voltage, built-in potential, dopant concentration, and depletion layer width of TSCs.

	V_{OC} [V]	V_{BI} [V]	V_{OC}-V_{BI} [V]	N [10^{14} cm^{-3}]
PffBT4T-2OD:$PC_{71}BM$	0.75	0.64	0.11	9.9
With 5% PCDTBT8	0.76	0.65	0.11	9.1
With 15% PCDTBT8	0.79	0.68	0.11	8.3
With 30% PCDTBT8	0.82	0.71	0.11	6.4